

Received August 14, 2018, accepted September 18, 2018, date of publication September 27, 2018, date of current version October 19, 2018.

Digital Object Identifier 10.1109/ACCESS.2018.2872391

Constrained Markov Decision Process Modeling for Sequential Optimization of Additive Manufacturing Build Quality

BING YAO[®] AND HUI YANG[®], (Senior Member, IEEE)

Complex System Monitoring, Modeling and Control Laboratory, The Pennsylvania State University, University Park Campus, State College, PA 16802, USA Corresponding author: Hui Yang (huy25@psu.edu)

This work was supported in part by the NSF Center for e-Design (Lockheed Martin) and in part by the NSF CAREER under Grant CMMI-1617148. The work of H. Yang was supported by the Harold and Inge Marcus Career Professorship.

ABSTRACT Additive manufacturing (AM) provides a greater level of flexibility to produce a 3-D part with complex geometries directly from the design. However, the widespread application of AM is currently hampered by technical challenges in process repeatability and quality control. To enhance the in-process information visibility, advanced sensing is increasingly invested for real-time AM process monitoring. The proliferation of *in situ* sensing data calls for the development of analytical methods for the extraction of features sensitive to layer-wise defects, and the exploitation of pertinent knowledge about defects for in-process quality control of AM builds. As a result, there are increasing interests and rapid development of sensor-based models for the characterization and estimation of layer-wise defects in the past few years. However, very little has been done to go from sensor-based modeling of defects to the suggestion of *in situ* corrective actions for quality control of AM builds. In this paper, we propose a new sequential decision-making framework for *in situ* control of AM processes through the constrained Markov decision process (CMDP), which jointly considers the conflicting objectives of both total cost (i.e., energy or time) and build quality. Experimental results show that the CMDP formulation provides an effective policy for executing corrective actions to repair and counteract incipient defects in AM before completion of the build.

INDEX TERMS Additive manufacturing, constrained Markov decision process, optimal control policy, quality control, defect mitigation.

I. INTRODUCTION

Additive manufacturing (AM) is a process to build complex 3D parts from computer-aided design (CAD) models through layer-upon-layer deposition of materials. AM provides significant advantages over traditional subtractive (machining) and formative (casting, molding) manufacturing processes, such as reducing material waste, eliminating specialized tooling cost, and enabling the creation of intricate and free-form geometries. It has been estimated that the global market for AM processes and services will reach around \$50 billion by the year of 2031 [1]. However, the widespread application of AM is currently hampered by technical challenges such as the lack of ability to realize real-time quality control. For example, process variations and uncertain factors significantly impact the microstructure and mechanical properties of AM builds, which will further lead to internal defects deteriorating the build hardness, strength, and residual stress.

Due to the high-level complexity of AM processes, advanced sensing systems (e.g., thermal camera, high-speed optical camera, photodetector, pyrometer, acoustic emission) are increasingly invested for real-time AM process monitoring and quality control. Advanced sensing brings a proliferation of complex-structured data with nonlinear and nonstationary patterns. Realizing full potentials of in-situ sensing data depends on the development of analytical methods for the extraction of features sensitive to layer-wise defects, and the exploitation of pertinent knowledge about defects for in-process quality control of AM builds. As a result, there are increasing interests and rapid development of sensor-based models for the characterization and estimation of layer-wise defects in the past few years. However, very little has been done to go from sensor-based modeling of defects to the suggestion of in-situ corrective actions for quality control of AM builds.



Indeed, the ability to mitigate incipient defects is critical to mandating stringent standards for both product esthetics and functional integrity in AM industries. The hybrid AM machines provide an opportunity to take corrective actions and improve the quality of AM build [2]. For example, if an AM layer is highly defective (i.e., with a high probability to contain defects), the hybrid machine can take an action to remove such layers (i.e., machining off the highly defective layer, denoted as a_M). If a layer has defects due to lack of fusion, the laser can be used to re-fuse and mitigate such defects (i.e., denoted as a_L). If an AM layer is with the low defect level (i.e., with a small probability to contain defects), the process will continue and no corrective action is taken (i.e., wait and do nothing, denoted as a_W). The choice of corrective actions will affect the evolving dynamics of defect states of the next layer and, through that, all subsequent layers, as illustrated in Fig. 1. Sequential optimization of AM processes is urgently needed to consider the uncertainty in transitions from layer to layer and minimize the expected cumulative cost through all layers.

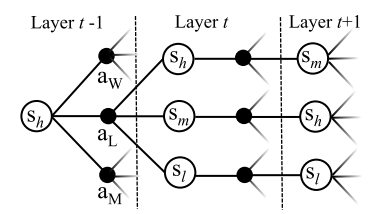


FIGURE 1. An illustration of state-action transition diagram. Note that s_h , s_m , and s_l denote the high, median, and low defect states of an AM layer.

However, sequential optimization of AM builds is a challenging task because of **conflicting criteria**, i.e., minimizing total energy (or time) cost consumed in the manufacturing process and maximizing the quality of final builds. For example, if corrective actions are taken too often, the total cost will be high although the build quality reaches the satisfactory level. If we decrease the frequency to take corrective actions, less energy will be consumed and, equivalently, the time to complete the build will be shortened, but there is a higher probability to yield a defective build. Very little has been done to develop an optimal sequential decision-making strategy for AM control with the consideration of conflicting objectives in both energy (or time) and quality. There is an urgent need to develop new decision-making models that help sequentially

optimize the quality of AM builds while minimizing the cost in energy (or time).

This paper presents a constrained Markov decision process (CMDP) framework to sequentially optimize AM processes by minimizing the total cost and, at the same time, controlling the quality of AM builds. Specifically, we model the variation of layer-wise defect index as a stochastic process to capture the evolving dynamics of AM defects. The defect state and corrective action in each layer will impact the defect condition of the next layer and, through that, all subsequent layers. Therefore, we propose a CMDP framework for the sequential optimal control of AM processes. The CMDP model is further utilized to derive an optimal control policy based on the series of defect-state index estimated from layer-wise images in a metal AM application. Experimental results show that layer-wise AM defects are effectively controlled under the CMDP policy, i.e., being mitigated before they reach the non-recoverable stage.

The rest of this paper is organized as follows: Section II introduces the research background of sensor-based monitoring and control of AM processes. Section III presents the research methodology that integrates sensor-based defect estimation with the CMDP framework for sequential AM optimization. Section IV shows the numerical experiments. Section V concludes this paper.

II. RESEARCH BACKGROUND

A. SENSOR-BASED MONITORING OF AM PROCESSES

In current practice, the quality of an AM build is commonly examined by post-build inspection techniques such as X-ray computed tomography (XCT) and scanning optical microscopy [3]–[5]. Such post-build inspection is well known to be expensive and time-consuming, and is not applicable for online quality control. The lack of in-situ quality assurance in AM parts hinders the widespread application of AM processes. Therefore, modern industries are increasingly investing in advanced sensing systems to cope with the high-level complexity of AM processes.

As shown in Table 1, there are a number of sensing systems developed for AM process monitoring, including optical camera, thermal camera, photodetector, pyrometer, acoustic emission, and optical emission. Foster *et al.* [6] developed an optical layer-wise imaging system to monitor the laser-powder-bed-fusion (LPBF) AM process in the Center for

TABLE 1. Sensing systems and analytical methods for defect detection in LPBM AM.

Sensing Systems	Data Types	Analytical Methods	
Optical camera [6], [17], [18]:	Optical image	Line-to-continuum [19], [20]	
Thermal camera [8], [21], [22]:	Thermal image	Self-organizing maps [23]	
Photodetector [12]:	Time series	Spectral graph theory [24]	
Pyrometer [9]:	3D point cloud	Multifractal analysis [25], [26]	
Acoustic emission [10]:	CAD design	Greedy Bayesian estimation [27]	
Optical emission [11]:	CT-scans	Statistical predictive modeling [28]	



Innovative Metal Processing through Direct Digital Deposition (CIMP-3D) at the Pennsylvania State University. This imaging system consists of a 36.3 megapixel DSLR camera that is placed inside the chamber of EOS M280 machine. It has been further implemented to identify and characterize defects caused by lack-of-fusion in the LPBF process [7]. Krauss *et al.* [8] proposed a real-time thermographic system using infrared cameras to monitor the selective laser melting process. This thermal system is implemented for layer-wise monitoring of the dynamic temperature distribution to identify hot spots in the early stage, which helps to avoid process interrupts.

In addition to imaging systems, Furumoto *et al.* [9] developed an in-situ system to monitor the layer-wise surface temperature using a two-color pyrometer in selective laser sintering and selective laser melting processes. Wang *et al.* [10] presented in-situ monitoring approach using the acoustic emission technique to investigate the crack generation and propagation during laser cladding process. Liu *et al.* [11] proposed a real-time sensing system using the optical emission spectrometer to monitor the temperature of the molten pool in the laser hot-wire cladding process. Lane *et al.* [12] combined an array of photodetector sensors with a thermal camera to investigate process variations in LPBF AM. For a comprehensive review of metal-based AM sensing system, see, e.g., [13]–[16].

B. SENSOR-BASED CHARACTERIZATION AND IDENTIFICATION OF AM DEFECTS

Advanced sensing brings a large amount of complexstructured data with nonlinear and nonstationary patterns. There is an urgent need to develop analytical methods for the extraction of features sensitive to layer-wise defects in AM builds. Recently, there are increasing interests in the development of sensor-based models to extract effective and sensitive features from the big sensing data to identify and characterize layer-wise defects in AM builds. Montazeri et al. [24] proposed a spectral-graph approach to study the photo-detector sensor signature for the identification of defects caused by material cross-contamination in LPBF AM process. Dunbar and Nassar [19] proposed a line-to-continuum approach to investigate the relation between process settings, sensor outputs, and build quality in PBF-AM using the optical emission spectroscopy. This approach has also been implemented for defect detection in the directed energy deposition (DED) processes [20].

In addition, Khanzadeh *et al.* [23] studied the melt-pool images and developed self-organizing maps to predict porosity in DED processes. Yao *et al.* [25] and Imani *et al.* [29] developed a multifractal analysis approach to identify and characterize layer-wise defect states from the surface images in LPBF-AM builds. Liu *et al.* [30] proposed an augmented Gaussian Cox process model to study the CT-scan images and quantify the layer-wise evolution of porosity in AM parts. Gobert *et al.* [31] utilized the support vector machine to extract multi-dimensional defect features from layer-wise

images captured by a high-resolution DSLR camera. Vandone *et al.* [32] proposed a multisensor approach to combine melt pool images with the 3D geometry from offline quality inspection for the DED process modeling.

Sensor-based models provide effective and sensitive features to identify and characterize layer-wise defects in AM builds, but are less concerned about in-situ corrective actions for the closed-loop control of AM processes. The defect condition and corrective action taken at each layer will significantly affect the next layer and all subsequent layers. Thus, there is an urgent need to develop a sequential strategy to account for the uncertainty in transitions from layer to layer and optimize the AM build quality.

C. AM PROCESS CONTROL

Rapid advances in sensing systems facilitate the development of new methods for AM process modeling and control, including the ON/OFF controller [33], proportional-integralderivative (PID) controllers [34], and a fuzzy logic-based controller [35], which focuses on improving the geometrical characteristic of AM parts. Also, Song and Mazumder [36] proposed a predictive control strategy to track and stabilize the melt pool temperature to a reference temperature profile in a laser cladding process. Craeghs et al. [37] built a feed-back controller using optical sensors to continuously monitoring the melt pool and optimize process parameters in the layer-wise laser melting process. Most of existing works focus on the modeling of defect conditions and process parameters (i.e., laser power, deposition thickness, hatch spacing), as well as the selection and stabilization of process parameters for the AM build. Those methods are less concerned about the uncertainty in the evolving dynamics of defect states from layer to layer, and do not account for the sequential decision making to mitigate incipient defects in AM processes.

The hybrid AM machines provide a set of corrective actions (e.g., machining-off, laser re-fusion) for the mitigation of AM defects in real-time before the completion of the build. Such corrective actions are different from the adjustment of process parameters. Rather, they provide an opportunity to repair a layer before proceeding to the next layer under the condition that process parameters are already set to be optimal. Note that Yao et al. [38] proposed a Markov decision process (MDP) framework to sequentially optimize the PBF AM process. However, the existing MDP models focus on a single objective and do not specifically consider the conflicting criteria in AM, i.e., minimizing total energy (or time) cost consumed in the manufacturing process and maximizing the quality of final builds. Little has been done to develop an optimal sequential strategy by considering the conflicting objectives in both energy and quality.

III. RESEARCH METHODOLOGY

This section presents a sequential framework of constrained Markov decision process (CMDP) to control the quality of AM builds. As shown in Fig. 2, we first extract defect



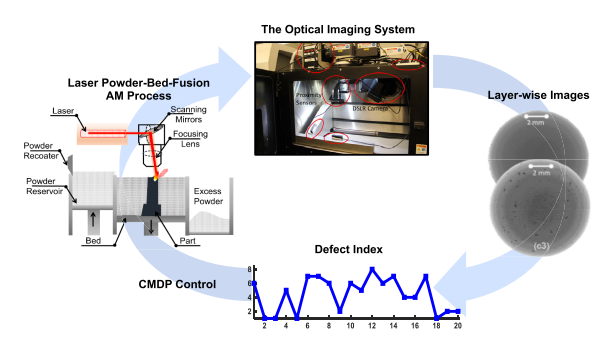


FIGURE 2. Flow diagram of the research methodology.

features from the layer-wise AM images captured by the optical imaging system developed in the CIMP-3D at Penn State [6]. Second, we model the evolving dynamics in the defect condition of AM layers using as a Gaussian process. Finally, we derive the optimal AM control policy through a CMDP framework by considering both energy (or time) cost and build quality. The effective AM process monitoring and build quality control are vertical steps to mitigate incipient defects, reduce rework rates, and further guarantee the economic viability of AM.

A. SENSOR-BASED MODELING OF AM DEFECTS

As shown in Table 1, a variety of analytical methods have been developed to analyze in-situ sensor data from AM processes and extract features that are sensitive to the layer-wise defects. Let $\boldsymbol{\theta}_t = [\theta_{t1}, \theta_{t2}, \ldots, \theta_{tp}]$ denote the vector of defect features, where $t \in \{1, 2, \ldots, T\}$ is the layer index, and p is the dimensionality of feature vector. Generally, it is assumed that $\boldsymbol{\theta}_t$ approximately follows the multivariate normal distribution, i.e., $\boldsymbol{\theta}_t \sim \mathcal{N}_p(\boldsymbol{\mu}, \Sigma_0)$, if the process is in control. Here, we propose to compute the composite index to represent the layer-wise defect condition as:

$$s_t = (\boldsymbol{\theta}_t - \bar{\boldsymbol{\theta}})' \Sigma^{-1} (\boldsymbol{\theta}_t - \bar{\boldsymbol{\theta}})$$
 (1)

where $\bar{\theta}$ is the sample mean and Σ is the sample variance. The defect index s_t simultaneously accounts for multi-dimensional variations among the defect conditions of layer t. The layer-wise structure of AM build then leads to a sequence of defect states in the form of stochastic signals as illustrated in Fig. 3. Given a large sample size, s_t approximately follows a χ_p^2 distribution if the dimensionality of features p > 10.

Further, we define the defect state by equiprobable division of the distribution of defect index s_t into l bands, as shown in Fig. 3. The breakpoints for l equiprobable bands are defined as a sorted list of boundary values $B = \{\beta_1, \beta_2, \ldots, \beta_{l-1}\}$ such that the area under the density curve between β_i and β_{i+1} is 1/l. For the distribution of $\chi^2_{p=20}$, the breakpoints for three equiprobable bands (i.e., l=3) are $\beta_1 = \chi^2_{1/3,p=20} = 16.7884$ and $\beta_2 = \chi^2_{2/3,p=20} = 22.1331$. Table 2 lists the breakpoints β 's for different number of equiprobable bands l. This results in the defect state space,

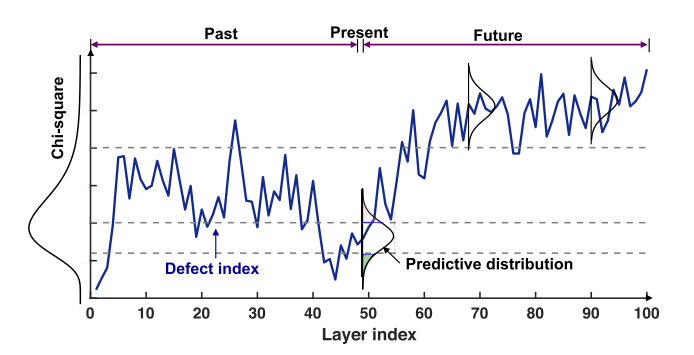


FIGURE 3. Stochastic dynamics in the series of layer-wise defect index.

TABLE 2. A lookup table of breakpoints that divides $\chi^2_{p=20}$ into different number (from 3 to 5) of equiprobable regions.

Breakpoints	l=3	l=4	l=5
$\beta = 1$	16.7884	15.4518	14.5784
$\beta = 2$	22.1331	19.3374	17.8088
$\beta = 3$		23.8277	20.9514
$\beta = 4$			25.0375

 $\mathcal{D} = \{d_1, \dots, d_l\}$, and the defect state at layer t is d_i if the defect index s_t falls into the band $[\beta_{i-1}, \beta_i)$. Note that d_1 represents the lowest defect level, and d_l denotes the highest defect level.

In addition, we model the evolving dynamics underlying the layer-wise defect states as Gaussian process. The predictive model is constructed by taking into account previous observations of the defect state. Specifically, the model input is defined as $\omega_t = [s_{t-\tau}, s_{t-\tau+1}, \dots, s_{t-1}]$, and s_t is the model output, i.e.,

$$s_t = f(\omega_t) + \epsilon, \quad t = 1, 2, 3, \dots$$
 (2)

where $f(\cdot)$: $\mathbb{R}^{\tau} \to \mathbb{R}$ is an unknown scalar function with a multi-dimensional input vector $\boldsymbol{\omega}_t \in \mathbb{R}^{\tau}$, and $\boldsymbol{\epsilon} \sim N(0, \sigma^2)$ denotes the Gaussian noise with zero mean and variance σ^2 . The task is to infer the unknown function $f(\cdot)$ given the input and noise observations.

For a collection of inputs: $\mathbf{\Omega} = [\boldsymbol{\omega}_1^T, \boldsymbol{\omega}_2^T, \dots, \boldsymbol{\omega}_n^T]^T$, there is a corresponding functional random variables: $f = [f_1, f_2, \dots, f_n]^T$, whose joint probability distribution is assumed to be Gaussian distribution, i.e.,

$$f|\Omega \sim N(\bar{f}, K)$$
 (3)

where \bar{f} is the mean function, and K is the covariance matrices, and is generally assumed to be in the form of squared exponential to guarantee that cases with nearby inputs will have highly correlated outputs. The hyper-parameters in Eq.(3) are given by the maximum likelihood estimation.

Given the observation history of defect index $s_- = \{s_1, s_2, \dots, s_{t-1}\}$ and the corresponding input Ω_- , prediction



of the distribution of s_t is expressed as

$$\begin{bmatrix} s_{-} \\ s_{t} \end{bmatrix} \sim \mathcal{N}\left(\begin{bmatrix} \bar{f}_{-} \\ \bar{f}_{t} \end{bmatrix}, \begin{bmatrix} K(\mathbf{\Omega}_{-}, \mathbf{\Omega}_{-}) + \sigma^{2}I & K(\mathbf{\Omega}_{-}, \boldsymbol{\omega}_{t}) \\ K(\boldsymbol{\omega}_{t}, \mathbf{\Omega}_{-}) & K(\boldsymbol{\omega}_{t}, \boldsymbol{\omega}_{t}) \end{bmatrix}\right)$$

The predictive distribution of s_t is given by

$$s_t \sim \mathcal{N}(\mu_{s_t}, \sigma_{s_t}^2) \tag{4}$$

where

$$\mu_{s_t} = \bar{f}_t + K(\boldsymbol{\omega}_t, \boldsymbol{\Omega}_-)[K(\boldsymbol{\Omega}_-, \boldsymbol{\Omega}_-) + \sigma_n^2 I]^{-1}(s_- - \bar{f}_-)$$

$$\sigma_{s_t}^2 = K(\boldsymbol{\omega}_t, \boldsymbol{\omega}_t) - K(\boldsymbol{\omega}_t, \boldsymbol{\Omega}_-)[K(\boldsymbol{\Omega}_-, \boldsymbol{\Omega}_-) + \sigma_n^2 I]^{-1}K(\boldsymbol{\Omega}_-, \boldsymbol{\omega}_t)$$

The transition probability in the defect state space from layer t-1 to layer t is then defined as:

$$P(d_t = d_j | d_{t-1} = d_i) = \phi \left(\frac{\beta_j - \mu_{d_j | d_i}}{\sigma_{d_i | d_i}^2} \right) - \phi \left(\frac{\beta_{j-1} - \mu_{d_j | d_i}}{\sigma_{d_i | d_i}^2} \right)$$

where $s_t \in [\beta_{j-1}, \beta_j) \sim d_j$, and ϕ is the cumulative density function of the standard normal distribution. The prediction model is utilized to recursively update the distribution of defect index s_t and to further develop the CMDP framework for sequential AM control.

B. CONSTRAINED MDP MODELING OF AM PROCESSES

Markov decision process (MDP) helps to derive the optimal policy by minimizing the expected cumulative cost or maximizing expected rewards for a sequential decision-making problem in the stochastic environment. The MDP has been used previously to sequentially optimize the maintenance of engineering systems [39], [40]. Note that the MDP framework commonly focuses on a single objective, and is less concerned about conflicting objectives as in the AM processes (i.e., minimizing total cost - energy or time, as well as maximizing the build quality). Hence, there is an urgent need to develop multi-objective optimization models for handling the sequential decision-making problem in AM control.

Constrained-MDP (CMDP) is an efficient approach for sequential optimization with the considering of conflicting objectives [41]. It has been previously implemented for risk analysis in finance [42] and path planning in vehicle swarm coordination problem [43], but very little has been done for the quality control of AM processes. In this paper, we propose a new CMDP framework to determine the optimal policy that minimizes the total energy (or time) cost and guarantees the quality of AM builds. The CMDP formulations are described as follows:

1) STATE SPACE

The state space is defined as $S = (T, \mathcal{D})$, where $T = \{1, 2, ..., T\}$ is the set of layer index, and \mathcal{D} is the set of defect states, i.e., $d_1, ..., d_l$, which is structured in the increasing order of defect levels (i.e., d_1 is the lowest defect level, and d_l denotes the highest defect level).

2) ACTION SPACE

The action space is defined as $\mathscr{A} = \{a_M, a_L, a_W\}$, where a_M denotes the action of machining off a layer with the cost of c_M , a_L is the action of laser re-fusion with the cost of c_L , and a_W represents the action of waiting (i.e., doing nothing) with the cost of c_W .

3) DECISION POLICY

The decision rule at layer t is denoted by $Q_t(d_t, a)$, which is defined as the probability of selecting action $a \in \mathcal{A}$ given the defect state d_t at layer index t.

4) STATE TRANSITION

Let $P_t^a(d_{t+1}|d_t)$ be the transition probability from state d_t of layer t to state d_{t+1} of layer t+1 under the action $a \in \mathcal{A}$. Given the decision policy $Q_t(d_t, a)$, the state transition is then defined as

$$M_t(i,j) = \sum_{a \in \mathcal{A}} Q_t(d_t, a) P_t^a(d_{t+1} = d_j | d_t = d_i)$$
 (5)

Let the vector $\mathbf{x}_t = [x_{t1}, \dots, x_{tl}]^T (\mathbf{1}^T \mathbf{x}_t = 1$, where 1 is a vector of 1's) represent the probability distribution of defect states $d_t \in \{d_1, \dots, d_l\}$ at layer t, which means the probability of defect index s_t staying in the defect state d_i is x_{ti} . Then, \mathbf{x}_t evolves according to:

$$\boldsymbol{x}_{t+1} = \boldsymbol{M}_t \boldsymbol{x}_t \tag{6}$$

The CMDP model is formulated as follows:

$$\min_{Q_1, \dots, Q_{T-1}} v_T = E_{x_1} \left[\sum_{t=1}^{T-1} c_t(x_t, Q_t) + c_T \right]
s.t. x_t \le h, \quad \mathbf{1}^T x_t = 1
x_{t+1} = M_t x_t, \quad Q_t \mathbf{1} = 1, \ Q_t \ge 0
\text{for } t = 1, 2, \dots, T-1$$
(7)

where Q_t is the decision matrix for layer t, v_T is the expected total cost in energy or time, $c_t(x_t, Q_t) = \sum_{a \in \mathscr{A}} c_a Q_t(d_t, a)$ is the immediate cost at layer t, and c_T is the terminal cost at the final layer T. The first set of constraints guarantees that the probability of each defect state is bounded by a predefined upper bound h and $0 \le h \le 1$. The last two sets of constraints guarantee each row of Q_t to be a valid probability distribution.

C. DYNAMIC PROGRAMMING TO SOLVE CMDP

If the upper-bound constraint (i.e., $x_t \le h$) is deleted in the CMDP model of Eq. (7), then the rows of Q_t are independent and not correlated. As such, the CMDP model can be solved by dynamic programming with simple backward induction. However, due to the upper-bound constraint on the distribution of defect density, the rows of Q_t are correlated in the formulation through state transition in Eq. (6). As a result, simple backward induction is not applicable here to solve the CMDP model.

In this subsection, we provide a feasible control policy by solving the CMDP model using dynamic programming for



the worst-case scenario of initial distribution of defect states. Specifically, the algorithm is summarized as follows:

- Step 1: Set the cost vector of defect states at layer T as $U_T = c_T$
- *Step 2*: For t = T 1, ..., 1, given U_{t+1} , compute the control policy for layer t by solving

$$\hat{Q}_{t} = \arg\min_{Q} \max_{\mathbf{x}} \mathbf{x}^{T} \left(\sum_{a} c_{a} Q(d_{t}, a) + M_{t}(Q)^{T} U_{t+1} \right)$$

$$s.t., \ 0 \le \mathbf{x} \le \mathbf{h}$$

$$M_{t}(Q)\mathbf{x} \le \mathbf{h}$$

$$\mathbf{1}^{T} \mathbf{x} = 1, \quad Q\mathbf{1} = \mathbf{1}, \ Q \ge 0$$
 (8)

The cost vector of defect states at layer t is

$$U_t = \sum_{a} c_a Q(d_t, a) + M_t(Q)^T U_{t+1}$$

• Output: control policy $\pi^* = \{\hat{Q}_1, \hat{Q}_2, \dots, \hat{Q}_{T-1}\}$ and the expected total cost $v_T^* \leq x_1^T U_1$.

Theorem 1: The control policy derived from the above algorithm guarantees that the expected total energy or time cost is smaller than an upper bound, i.e., $v_T^* \leq \mathbf{x}_1^T U_1$.

cost is smaller than an upper bound, i.e., $v_T^* \leq x_1^T U_1$.

Proof: We define $g_T(x_T) = x_T^T U_T$ (i.e., the expected cost when t = T), and the expected cost at t is defined as $g_t(x_t) = \min_{Q_t} \{x_t^T c_t(x_t, Q_t) + g_{t+1}(M_t x_t)\}$. Therefore, the expected total cost for the whole process is $v_T = g_1(x_1)$ through the backward accumulation. Next, we will prove $g_t(x_t) \leq x_t^T U_t$ by mathematic induction. Because the upper bound $g_T(x_T) \leq x_T^T U_T$ is true for t = T, if it is also true for t + 1, i.e., $g_{t+1}(x_{t+1}) \leq x_{t+1}^T U_{t+1}$, then we have

$$\begin{split} g_{t}(\boldsymbol{x}_{t}) &= \min_{Q_{t}} \{\boldsymbol{x}_{t}^{T} c_{t}(\boldsymbol{x}_{t}, Q_{t}) + g_{t+1}(M_{t}\boldsymbol{x}_{t})\} \\ &\leq \min_{Q_{t}} \{\boldsymbol{x}_{t}^{T} c_{t}(\boldsymbol{x}_{t}, Q_{t}) + \boldsymbol{x}_{t}^{T} M_{t}^{T} \boldsymbol{U}_{t+1}\} \\ &= \min_{Q_{t}} \{\boldsymbol{x}_{t}^{T} (c_{t}(\boldsymbol{x}_{t}, Q_{t}) + M_{t}^{T} \boldsymbol{U}_{t+1})\} \\ &= \min_{Q_{t}} \{\boldsymbol{x}_{t}^{T} (\sum_{a} c_{a} Q(d_{t}, a) + M_{t}(Q)^{T} \boldsymbol{U}_{t+1})\} \\ &= \min_{Q_{t}} \{\boldsymbol{x}_{t}^{T} \boldsymbol{U}_{t}\} \leq \boldsymbol{x}_{t}^{T} \boldsymbol{U}_{t} \end{split}$$

According to mathematic induction, we have $v_T^* = g_1(x_1) \le x_1^T U_1$, which completes the proof.

D. DERIVATION OF Q_t BY LINEAR PROGRAMMING DUAL THEORY

The computation of Q_t in Eq. (8) pose a significant challenge on implementing the proposed backward dynamic programming to solve the CMDP model. Note that the formulation of min-max linear programming (LP), due to the interaction term of $M_t(Q)x$, cannot be simply solved by the conventional min-max LP algorithms. In this subsection, we will detail how to solve Q_t using the LP dual theory.

Theorem 2: If the min-max LP problem in Eq. (8) is transformed into the equivalent LP formulation below:

$$\min_{Q,\mathbf{y},z,\mathbf{w},F} \mathbf{h}^T \mathbf{y} + z$$

$$s.t., \ \mathbf{y} + z\mathbf{1} \ge U_t(Q)$$

$$(M(Q) - \mathbf{w}\mathbf{1}^T + \Gamma)\mathbf{h} + \mathbf{w} \le \mathbf{h}$$

$$- \mathbf{w}\mathbf{1}^T + \Gamma + M(Q) \ge 0$$

$$Q\mathbf{1} = \mathbf{1}$$

$$\mathbf{y}, \Gamma, Q \ge 0, \ z \text{ unconstrained} \tag{9}$$

Then, the control policy Q_t is obtained.

Proof: If we define $\mathbf{b} = \mathbf{U}_t$, $A = (\mathbf{I}, 1, -1)$, $\mathbf{k}^T = (\mathbf{h}^T, 1, -1)$, the max LP in Eq. (8) can be represented as:

$$\max \mathbf{b}^T \mathbf{x}$$
s.t., $A^T \mathbf{x} < \mathbf{k} \quad \mathbf{x} > 0$ (10)

The corresponding dual problem becomes

min
$$h^T y + z$$

 $s.t., y + z\mathbf{1} \ge U_t(Q)$
 $y \ge 0, z \text{ unconstrained}$ (11)

Considering arg min in Eq. (8), the allowable domain of Q can be represented by linear inequalities so as to formulate a minimization LP problem. Note that the probability upper bound of each defect state holds if and only if the following condition holds:

$$\max_{\mathbf{x}_t \le \mathbf{h}, \mathbf{1}^T \mathbf{x} = 1} M_t(Q) \mathbf{x}_t \le \mathbf{h}$$
 (12)

which ensures that the probability distribution of defect states satisfies the upper-bound constraint at current layer t as well as at next layer t+1 after state transition.

The dual of the i^{th} LP in Eq. (12) is formulated as

min
$$h^T z' + w$$

 $s.t., z' + 1w \ge M^T(Q)e_i$
 $z' \ge 0, \quad w \text{ unconstrained}$ (13)

where e_i is a unit vector whose i^{th} element is 1. Adding the surplus variables γ and ρ , the LP in Eq. (13) becomes

min
$$h^T z' + w$$

s.t., $z' + \mathbf{1}w - \mathbf{\gamma} = M^T(Q)e_i$
 $z' - \rho = 0$
 $\rho \ge 0$, $\mathbf{\gamma} \ge 0$ w unconstrained (14)
 \Rightarrow
min $h^T (M^T(Q)e_i - \mathbf{1}w + \mathbf{\gamma}) + w$
s.t., $M^T(Q)e_i - \mathbf{1}w + \mathbf{\gamma} \ge 0$
 $\mathbf{\gamma} \ge 0$, w unconstrained (15)

According to the strong dual property, the optimal objective value of Eq. (15) equals to that of Eq. (12). Note that the optimal objective value of Eq. (12) satisfies the upper-bound constraint, which means the optimal value of Eq. (15) needs to



satisfy the same constraint, i.e, $h^T(M^T(Q)e_i - 1w + \gamma) + w \le h_i$. Thus, the LP problem in Eq (12) can be equivalently formulated as

$$(M(Q) - \mathbf{w}\mathbf{1}^{T} + \Gamma)\mathbf{h} + \mathbf{w} \le \mathbf{h}$$

$$M(Q) - \mathbf{w}\mathbf{1}^{T} + \Gamma \ge 0$$

$$Q\mathbf{1} = \mathbf{1}, \quad \Gamma, \ Q \ge 0 \quad (16)$$

Combining Eq. (16) with Eq. (11) completes the proof.

IV. NUMERICAL EXPERIMENTS

We implement the proposed CMDP framework to derive the optimal control policy for AM processes. The layer-wise imaging data are acquired from the LPBF process of an AM build as illustrated in Fig. 4(a). Each AM image is characterized by 7360×4912 pixels with a pixel size of $12.22\mu m$. The availability of in-situ data enables the extraction of defective features that are sensitive to the variations in quality characteristics of each layer in the build.



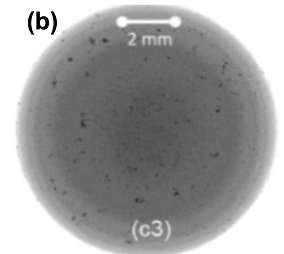


FIGURE 4. (a) The AM build by the LPBF-AM process; (b) The 2D image of an AM layer.

As aforementioned, sensor-based methods were developed to analyze in-situ AM data, characterize build defects, and extract the layer-wise defect index (i.e., s_t). The resulted continuous defect index s_t is then discretized into ten states using the equiprobable method as introduced in Section II.A. This leads to the defect state space, i.e., $\mathcal{D} = \{d_1, d_2, \dots, d_{10}\}$. Note that we use $1, 2, \dots, 10$ to denote the defect state d_1, d_2, \dots, d_{10} in Fig. 7.

Three actions are considered in this case study, i.e., a_M machining off, a_L - laser re-fusion, and a_W - wait and do nothing, with the corresponding cost of $c_M = 10$, $c_L = 4$, and $c_W = 1$. We define the terminal cost at the final layer as $c_T =$ [1, 1, 1, 1, 50, 50, 50, 100, 100, 1000] for the increase levels of defect states $d_1 \sim d_{10}$. In other words, we assign a relatively high terminal cost to the final layer that is with a higher probability of failure. If the defect state is no higher than d_4 , the cost is as small as 1. During the printing process, it is desirable to control the layer-wise build quality, i.e., reducing the probability of AM layers to enter high-defect states. As such, we define the probability upper bound as h =[1, 1, 1, 1, 0.1, 0.1, 0.1, 0.001, 0.001, 0.00001] for the defect states from d_1 to d_{10} . This definition guarantees that the probability of AM layers staying in state d_5 , d_6 , or d_7 should not exceed 0.1, and that in state d_8 (or d_9) and d_{10} should not be greater than 0.001 and 0.00001.

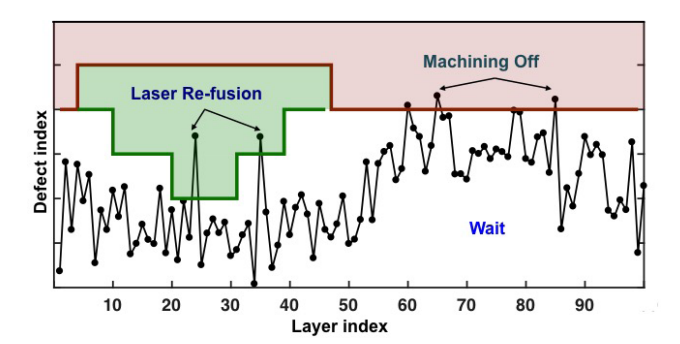


FIGURE 5. The optimal CMDP policy for AM quality control.

Fig. 5 shows the control policy derived from the proposed CMDP framework. Note that if the defect index s_t locates in the region below the green and red step curves, the optimal action is to wait and let the AM process continue operating (i.e., a_W). If s_t exceeds the green step curve and is in the green area, the action a_L is chosen to fuse the defective region again using the laser. Otherwise, if s_t is high and goes beyond the red step curve into the red region, the policy will choose the expensive but more effective action a_M , i.e., machining off the entire layer that is highly defective.

Fig. 6 shows the performance comparison between MDP and CMDP policies. Note that the average probability in the low-defect states (including d_1 , d_2 , d_3 , and d_4) over time under the CMDP policy is 0.9217 ± 0.0441 , which are significantly higher than that under the MDP policy 0.4948 ± 0.0315 . Moreover, the average probability in the median-defect state (including d_5 , d_6 , and d_7) and high-defect state (including d_8 and d_9) over the printing process under the MDP policy is 0.4452 ± 0.1068 and 0.0486 ± 0.0346 , respectively, both of which are much bigger than that under the proposed CMDP policy of 0.0781 ± 0.0161 and $1.6 \times 10^{-4} \pm 6.8 \times 10^{-5}$.

It may also be noted that the average probability to enter the highest defect state (i.e., d_{10}) is $2.3 \times 10^{-6} \pm 1.5 \times 10^{-6}$ during the building process under CMDP policy, which is much lower than 0.0114 ± 0.0073 under the MDP policy. If we assume the AM build fails whenever any of its layers goes beyond d_{10} , the failure probability under CMDP policy is $1-(1-2.3\times 10^{-6})^{100}=0.023\%$ for a 100-layer build, but is $1-(1-0.0114)^{100}=68\%$ under the MDP policy. Thus, the quality of AM builds is controlled more effectively and has a lower probability of failure under the CMDP policy than that under the MDP policy.

Fig. 7 shows the variations of CMDP policies with respect to the ratio of c_L (i.e., cost of a_L) over c_M (i.e, cost of a_M). Fig. 7(a) shows that the control limit of a_L increases as c_L/c_M increases, while that of a_M decreases as shown in Fig. 7(b). This is due to the fact that after the action a_M (i.e., machining off the entire layer), there will be a higher chance to enter the low-defect states than by fusing the layer again with laser. If the ratio c_L/c_M increases (i.e., the cost of laser re-fusion becomes comparable to the cost of machining off), the



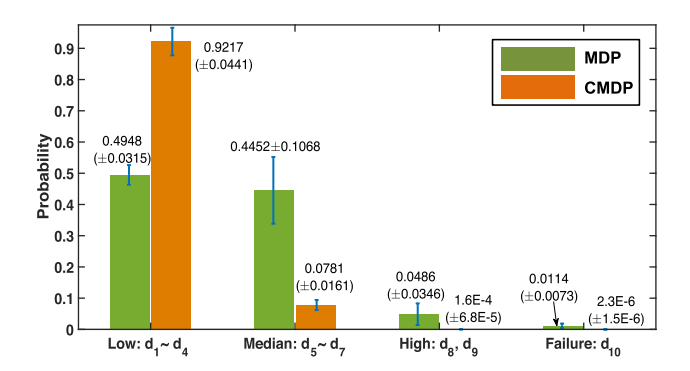
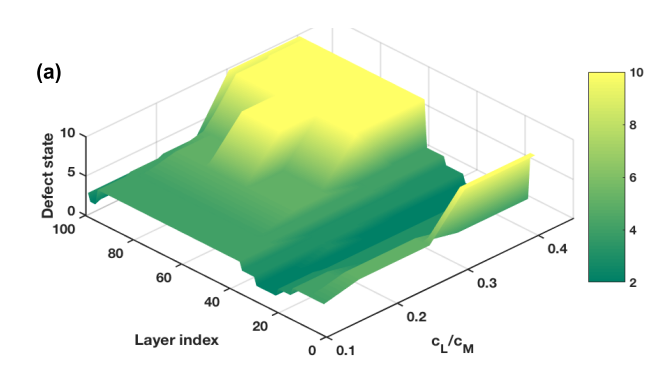


FIGURE 6. Performance comparison between MDP and CMDP policies.



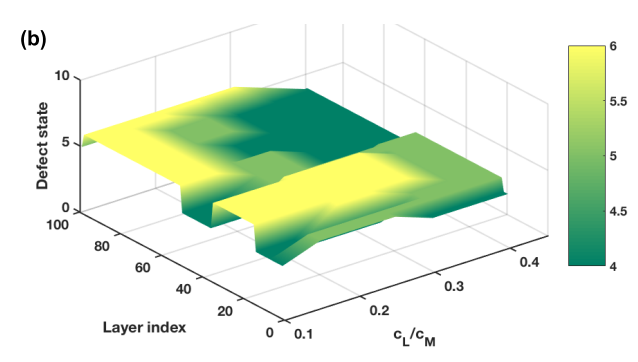


FIGURE 7. The variation of CMDP policy of taking (a) a_L (i.e., laser re-fusion) and (b) a_M (i.e., machining off) with respect to the cost ratio c_L/c_M .

optimal policy is to take the more-effective action a_M rather than taking the less-effective action a_L with a comparable cost.

V. CONCLUSIONS

In this paper, we formulate the in-situ AM quality control as a sequential decision-making problem through the CMDP framework. As sensor-based analytical methods have been developed to provide effective and sensitive defect features for each layer in the AM build, we propose to compute the composite index of defect characteristics in each layer that simultaneously considers multidimensional variations among these features. Further, we model and predict the stochastic evolving dynamics of defect states from one layer to the next as a Markov process. Then, we derive the sequential control

policy to optimize the build quality through the CMDP framework, which jointly considers the conflicting objectives of total cost (i.e., either energy or time) and build quality. Experimental results show that the CMDP formulation provides an effective policy for executing corrective actions to repair and counteract incipient defects in AM before completion of the build. The probability to contain embedded defects in the AM build is much smaller (i.e., 0.023% for a 100-layer build) than the traditional MDP policy (i.e., 68%). The proposed sequential optimization framework has great potentials for real-time defect mitigation and quality control of AM builds.

ACKNOWLEDGMENTS

The authors gratefully acknowledge the valuable contributions of Dr. Edward Reutzel and Dr. Abdalla Nassar from the CIMP-3D at Penn State for providing the data utilized in this research.

REFERENCES

- D. Thomas, "Costs, benefits, and adoption of additive manufacturing: A supply chain perspective," *Int. J. Adv. Manuf. Technol.*, vol. 85, nos. 5–8, pp. 1857–1876, 2016.
- [2] M. P. Sealy, G. Madireddy, R. E. Williams, P. Rao, and M. Toursangsaraki, "Hybrid processes in additive manufacturing," *J. Manuf. Sci. Eng.*, vol. 140, no. 6, p. 060801, 2018.
- [3] F. H. Kim, S. P. Moylan, E. J. Garboczi, and J. A. Slotwinski, "Investigation of pore structure in cobalt chrome additively manufactured parts using X-ray computed tomography and three-dimensional image analysis," *Additive Manuf.*, vol. 17, pp. 23–38, Oct. 2017.
- [4] I. Maskery et al., "Quantification and characterisation of porosity in selectively laser melted Al–Si10–Mg using X-ray computed tomography," Mater. Characterization, vol. 111, pp. 193–204, Jan. 2016.
- [5] P. Wang et al., "Scanning optical microscopy for porosity quantification of additively manufactured components," Additive Manuf., vol. 21, pp. 350–358, May 2018.
- [6] B. Foster, E. Reutzel, A. Nassar, B. Hall, S. Brown, and C. Dickman, "Optical, layerwise monitoring of powder bed fusion," in *Proc. Solid Freeform Fabr. Symp.*, 2015, pp. 295–307.
- [7] M. Abdelrahman, E. W. Reutzel, A. R. Nassar, and T. L. Starr, "Flaw detection in powder bed fusion using optical imaging," *Additive Manuf.*, vol. 15, pp. 1–11, May 2017.
- [8] H. Krauss, C. Eschey, and M. Zaeh, "Thermography for monitoring the selective laser melting process," in *Proc. Solid Freeform Fabr. Symp.*, 2012, pp. 999–1014.
- [9] T. Furumoto, T. Ueda, M. R. Alkahari, and A. Hosokawa, "Investigation of laser consolidation process for metal powder by two-color pyrometer and high-speed video camera," *CIRP Ann.-Manuf. Technol.*, vol. 62, no. 1, pp. 223–226, 2013.
- [10] F. Wang, H. Mao, D. Zhang, X. Zhao, and Y. Shen, "Online study of cracks during laser cladding process based on acoustic emission technique and finite element analysis," *Appl. Surf. Sci.*, vol. 255, no. 5, pp. 3267–3275, 2008.
- [11] S. Liu, W. Liu, M. Harooni, J. Ma, and R. Kovacevic, "Real-time monitoring of laser hot-wire cladding of Inconel 625," *Opt. Laser Technol.*, vol. 62, pp. 124–134, Oct. 2014.
- [12] B. Lane, E. Whitenton, and S. Moylan, "Multiple sensor detection of process phenomena in laser powder bed fusion," *Proc. SPIE*, vol. 9861, p. 986104, May 2016.
- [13] G. Tapia and A. Elwany, "A review on process monitoring and control in metal-based additive manufacturing," *J. Manuf. Sci. Eng.*, vol. 136, no. 6, p. 060801, 2014.
- [14] B. K. Foster, E. W. Reutzel, A. R. Nassar, C. J. Dickman, and B. T. Hall, "A brief survey of sensing for metal-based powder bed fusion additive manufacturing," *Proc. SPIE*, vol. 9489, p. 94890B, May 2015.
- [15] S. K. Everton, M. Hirsch, P. Stravroulakis, R. K. Leach, and A. T. Clare, "Review of *in-situ* process monitoring and *in-situ* metrology for metal additive manufacturing," *Mater. Des.*, vol. 95, pp. 431–445, Apr. 2016.



- [16] M. Grasso and B. M. Colosimo, "Process defects and in situ monitoring methods in metal powder bed fusion: A review," Meas. Sci. Technol., vol. 28, no. 4, p. 044005, 2017.
- [17] J. Jacobsmühlen, S. Kleszczynski, G. Witt, and D. Merhof, "Robustness analysis of imaging system for inspection of laser beam melting systems," in *Proc. Emerg. Technol. Factory Autom. (ETFA)*, Sep. 2014, pp. 1–4.
- [18] Y. Xiong, W. H. Hofmeister, Z. Cheng, J. E. Smugeresky, E. J. Lavernia, and J. M. Schoenung, "In situ thermal imaging and three-dimensional finite element modeling of tungsten carbide-cobalt during laser deposition," Acta Mater., vol. 57, no. 18, pp. 5419–5429, 2009.
- [19] A. J. Dunbar and A. R. Nassar, "Assessment of optical emission analysis for in-process monitoring of powder bed fusion additive manufacturing," *Virtual Phys. Prototyping*, vol. 13, no. 1, pp. 14–19, 2018.
- [20] C. B. Stutzman, A. R. Nassar, and E. W. Reutzel, "Multi-sensor investigations of optical emissions and their relations to directed energy deposition processes and quality," *Additive Manuf.*, vol. 21, pp. 333–339, May 2018.
- [21] B. Lane, S. Moylan, E. P. Whitenton, and L. Ma, "Thermographic measurements of the commercial laser powder bed fusion process at NIST," *Rapid Prototyping J.*, vol. 22, no. 5, pp. 778–787, 2016.
- [22] Y. Zhang, G. S. Hong, D. Ye, K. Zhu, and J. Y. H. Fuh, "Extraction and evaluation of melt pool, plume and spatter information for powderbed fusion AM process monitoring," *Mater. Des.*, vol. 156, pp. 458–469, Oct. 2018
- [23] M. Khanzadeh, S. Chowdhury, M. A. Tschopp, H. R. Doude, M. Marufuzzaman, and L. Bian, "In-situ monitoring of melt pool images for porosity prediction in directed energy deposition processes," IISE Trans., to be published.
- [24] M. Montazeri, R. Yavari, P. Rao, and P. Boulware, "In-process monitoring of material cross-contamination defects in laser powder bed fusion," *J. Manuf. Sci. Eng.*, vol. 140, no. 11, p. 111001, 2018.
- [25] B. Yao, F. Imani, A. S. Sakpal, E. W. Reutzel, and H. Yang, "Multifractal analysis of image profiles for the characterization and detection of defects in additive manufacturing," ASME J. Manuf. Sci. Eng., vol. 140, no. 3, p. 031014, 2018.
- [26] F. Imani, B. Yao, R. Chen, P. K. Rao, and H. Yang, "Fractal pattern recognition of image profiles for manufacturing process monitoring and control," in *Proc. 13th Int. Manuf. Sci. Eng. Conf.*, 2018, p. 1.
- [27] K. Bastani, P. K. Rao, and Z. Kong, "An online sparse estimation-based classification approach for real-time monitoring in advanced manufacturing processes from heterogeneous sensor data," *IIE Trans.*, vol. 48, no. 7, pp. 579–598, 2016.
- [28] Q. Huang, H. Nouri, K. Xu, Y. Chen, S. Sosina, and T. Dasgupta, "Statistical predictive modeling and compensation of geometric deviations of three-dimensional printed products," *J. Manuf. Sci. Eng.*, vol. 136, no. 6, p. 061008, 2014.
- [29] F. Imani, A. Gaikwad, M. Montazeri, P. Rao, H. Yang, and E. Reutzel, "Process mapping and in-process monitoring of porosity in laser powder bed fusion using layerwise optical imaging," *J. Manuf. Sci. Eng.*, vol. 140, no. 10, p. 101009, 2018.
- [30] J. Liu, C. Liu, Y. Bai, P. Rao, C. Williams, and Z. Kong, "Layer-wise spatial modeling of porosity in additive manufacturing," *IISE Trans.*, pp. 1–40, Jun. 2018.
- [31] C. Gobert, E. W. Reutzel, J. Petrich, A. R. Nassar, and S. Phoha, "Application of supervised machine learning for defect detection during metallic powder bed fusion additive manufacturing using high resolution imaging," *Additive Manuf.*, vol. 21, pp. 517–528, May 2018.
- [32] A. Vandone, S. Baraldo, and A. Valente, "Multisensor data fusion for additive manufacturing process control," *IEEE Robot. Autom. Lett.*, vol. 3, no. 4, pp. 3279–3284, Oct. 2018.
- [33] J. Mazumder, D. Dutta, N. Kikuchi, and A. Ghosh, "Closed loop direct metal deposition: Art to part," *Opt. Lasers Eng.*, vol. 34, nos. 4–6, pp. 397–414, 2000.
- [34] E. Toyserkani and A. Khajepour, "A mechatronics approach to laser powder deposition process," *Mechatronics*, vol. 16, no. 10, pp. 631–641, 2006.
- [35] Y. Hua and J. Choi, "Adaptive direct metal/material deposition process using a fuzzy logic-based controller," J. Laser Appl., vol. 17, no. 4, pp. 200–210, 2005.
- [36] L. Song and J. Mazumder, "Feedback control of melt pool temperature during laser cladding process," *IEEE Trans. Control Syst. Technol.*, vol. 19, no. 6, pp. 1349–1356, Nov. 2011.
- [37] T. Craeghs, F. Bechmann, S. Berumen, and J.-P. Kruth, "Feedback control of layerwise laser melting using optical sensors," *Phys. Procedia*, vol. 5, no. 2, pp. 505–514, 2010.

- [38] B. Yao, F. Imani, and H. Yang, "Markov decision process for image-guided additive manufacturing," *IEEE Robot. Autom. Lett.*, vol. 3, no. 4, pp. 2792–2798, Oct. 2018.
- [39] A. H. Elwany, N. Z. Gebraeel, and L. M. Maillart, "Structured replacement policies for components with complex degradation processes and dedicated sensors," *Oper. Res.*, vol. 59, no. 3, pp. 684–695, 2011.
- [40] M. Kurt and J. P. Kharoufeh, "Monotone optimal replacement policies for a Markovian deteriorating system in a controllable environment," *Oper. Res. Lett.*, vol. 38, no. 4, pp. 273–279, 2010.
- [41] M. L. Puterman, Markov Decision Processes: Discrete Stochastic Dynamic Programming. Hoboken, NJ, USA: Wiley, 2014.
- [42] V. Borkar and R. Jain, "Risk-constrained Markov decision processes," *IEEE Trans. Autom. Control*, vol. 59, no. 9, pp. 2574–2579, Sep. 2014.
- [43] M. El Chamie, Y. Yu, and B. Açıkmese, "Convex synthesis of randomized policies for controlled Markov chains with density safety upper bound constraints," in *Proc. Amer. Control Conf.*, Jul. 2016, pp. 6290–6295.



BING YAO received the B.S. degree in physics from the University of Science and Technology of China, Hefei, China, in 2012, and the M.S. degree in physics from The Pennsylvania State University, University Park Campus, State College, PA, USA, in 2015, where she is currently pursuing the Ph.D. degree with the Harold and Inge Marcus Department of Industrial and Manufacturing Engineering. Her research focuses on physical-statistical modeling and optimization of complex healthcare

and manufacturing systems.



HUI YANG is currently a Harold and Inge Marcus Career Associate Professor with the Harold and Inge Marcus Department of Industrial and Manufacturing Engineering, The Pennsylvania State University, University Park Campus, State College, PA, USA. His research program is supported by the National Science Foundation (including the prestigious NSF CAREER Award), Lockheed Martin, NSF Center for e-Design, NSF Center for Healthcare Organization Transforma-

tion, and equipment grants from NSF and State of Florida for laboratory computing infrastructure improvement. His research interests focus on sensor-based modeling and analysis of complex systems for process monitoring, process control, system diagnostics, condition prognostics, quality improvement, and performance optimization.

Dr. Yang has co-authored the book *Healthcare Analytics: From Data to Knowledge to Healthcare Improvement* (John Wiley & Sons, 2016). He is a Professional Member of IEEE, IEEE EMBS, INFORMS, IIE, ASEE, and American Heart Association. He served as the President of INFORMS Quality, Statistics and Reliability Society from 2015 to 2016 and the Program Chair of the 2016 Industrial and Systems Engineering Research Conference. Also, he served as the President of the IISE Data Analytics and Information Systems Society (2017 ~ 2018). He is an Associate Editor of the *IISE Transactions*, the IEEE Journal of Biomedical and Health Informatics, EEE Robotics and Automation Letters, *Quality Technology and Quality Management*, Proceedings of 2018 IEEE Conference on Biomedical and Health Informatics, Proceedings of 2018 IEEE International Conference on Automation Science and Engineering, and Proceedings of 2017 IEEE International Conference on Automation Science and Engineering.